

Raman lidar characterization using a reference lamp

Eduardo Landulfo^a, Renata F. da Costa^a, Patricia F. Rodrigues^a, Fábio J. da Silva Lopes^{a,b}

^aCentro de Lasers e Aplicações (CLA) - Instituto de Pesquisas Energéticas e Nucleares (IPEN-CNEN), Av. Prof. Lineu Prestes 2242, Cidade Universitária, CEP 05508-000, São Paulo-SP, Brasil;

^bInstituto de Astronomia, Geofísica e Ciências Atmosféricas (IAG) - Universidade de São Paulo (USP), Rua do Matão 1226, Cidade Universitária, CEP 05508-090, São Paulo-SP, Brasil;

ABSTRACT

The determination of the amount of water vapor in the atmosphere using lidar is a calibration dependent technique. Different collocated instruments are used for this purpose, like radiosoundings and microwave radiometers. When there are no collocated instruments available, an independent lamp mapping calibration technique can be used. Aiming to stabilize an independent technique for the calibration of the six channels Nd-YAG Raman lidar system located at the Center for Lasers and Applications (CLA), São Paulo, Brazil, an optical characterization of the system was first performed using a reference tungsten lamp. This characterization is useful to identify any possible distortions in the interference filters, telescope mirror and stray light contamination. In this paper we show three lamp mapping characterizations (01/16/2014, 01/22/2014, 04/09/2014). The first day is used to demonstrate how the technique is useful to detect stray light, the second one how it is sensible to the position of the filters and the third one demonstrates a well optimized optical system.

Keywords: Lidar calibration, Raman lidar, Water vapor

1. INTRODUCTION

The use of Raman Lidar is a well established technique for atmospheric species concentration determination.¹⁻⁵ In comparison with other techniques, such as DIAL, Raman can give a direct measurement of the mixing ratio of the species being probed, for example in the case of the water vapor mixing ratio determination we need to know the backscattering Raman signal from water vapor and nitrogen or oxygen as reference gases.

Moreover in order to get reliability in the measurement and accuracy assessment the Raman Lidar system should go through a calibration process analysis as fully documented many efforts have been performed to obtain a system calibration.⁶⁻¹³ In general these calibration methodologies started at looking for a smaller uncertainty and independent procedures to calibrate a Raman Lidar system for water vapor measurements and relied on accurate theoretical cross section calculations or their direct application in water vapor raman lidar measurements.¹⁴⁻¹⁷ In addition, more recent papers used this methodology to calibrate others systems that not only operated under the rules of Raman scattering but with a broader spectroscopic based system¹⁸⁻²⁰ which showed other pathways to use this approach not only for means of calibration but also for characterising the optical system being employed to carry out a specific experiment.

In this paper we present a methodology to verify the performance of a 6-channel lidar system based on a scanning calibrated lamp. The whole analysis was made in 3 steps when a first scan was made and some *mis performances* were detected related to stray light, then after correcting this issue a second run was made which allowed us to identify a misalignment in one of the channels and again after correcting we made the last run and optimize the filter selection for each channel in a way to get the best signal-to-noise ratio (SNR) possible. The results showed a lot of consistency and helped to identify issues in the optical system making it clear that the calibration method could be also used as an ameliorating procedure to enhance a system optical response.

Further author information: (Send correspondence to Dr. Eduardo Landulfo)
Dr. Eduardo Landulfo: E-mail: elandulf@ipen.br, Telephone: +55 11 3133 9372

2. METHODOLOGY

2.1 System Setup

The lidar system called MSP-Lidar I, is located at Centro de Lasers e Aplicaes (CLA) from the Instituto de Pesquisas Energticas e Nucleares (IPEN $-23^{\circ} 56' S$, $46^{\circ} 74' W$, 740 m above sea level), in the western region of So Paulo. The MSP-Lidar is a multiwavelength Raman lidar operating at CLA since 2001.^{21,22} It is configured in a monostatic biaxial alignment pointing vertically to the zenith.

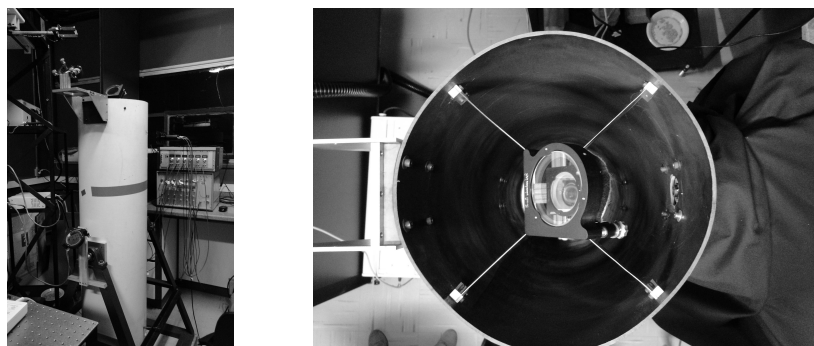


Figure 1. Lidar system used to this experiment. On the right, the mapped area of the telescope.

The laser beam has an average diameter of 9 mm and is directed to a beam expander (expands the three wavelengths), which increases the beam diameter about 5 times, with a divergence of less than 0.1 mrad. The expanded laser beam is then directed to the atmosphere through a second set of mirrors (periscope).

A 30 cm diameter telescope (Focal length of 1.5 m) is used to collect the backscattered laser light. The telescope's field of view (FOV) can be adjusted until a desirable value of 0.1 mrad is reached, using a small diaphragm. The system is currently used with a fixed FOV of 0.1 mrad, which permits a full overlap between the telescope FOV and the laser beam at altitudes higher than 1000 m above the ground level. This FOV value, in accordance with the detection electronics, permits the probing of the atmosphere up to the free troposphere.

Table 1. Sumarized Setup of the MSP-LIDAR I

Laser	
Laser type	Nd:YAG Laser (Brilliant B by Quantel)
Wavelengths	355, 532 nm
Pulse energy	230 mJ (355 nm), 400 mJ (532 nm)
Repetition rate	10 Hz
Pulse duration	6 ns
Receiver	
Optical design	30-cm diameter Newtonian telescope
Focal length	1.5 m
Field of view	0.1 mrad
Transient recorder	Licel TR20-80/ TR20-160/ TR20-40
Photoncounting count rate	250 MHz

The detection box collects six different wavelengths and separates them into six different channels (the elastic 355 nm and the corresponding shifted Raman signals: nitrogen 387 nm, and water vapor, 408 nm; the elastic 532 nm and the corresponding shifted Raman signals: nitrogen 607 nm and water vapor 660 nm) using a combination of high-pass and low-pass filters. Each splitted bean is directed to narrowbands spectral interference filters (532 ± 1.0 nm FWHM, 355 ± 1.0 nm FWHM, 387 ± 0.25 nm FWHM, 408 ± 0.25 nm FWHM 607 ± 0.25 nm FWHM, 660 ± 0.25 nm FWHM) and then directed to photomultipliers tubes (PMTs). R7400 photomultiplier

tubes from Hamamatsu are used for all channels, except for 607 and 660 nm, where R9880U-20 are used. The R9880U-20 has a better quantum efficiency (around 20%) at range 550 - 700 nm, improving the signal to noise ratio of the weak Raman signal at these wavelengths.

The PMT signals are digitized by a transient recorder TR 20-80/160 for 532 nm, TR 20-160 for 355, 387 and 408 nm, TR 20-40 for 607 and 660 nm, all supplied by LICEL. They are recorded in both analog and photoncounting mode. Table 1 summarized the setup system for this study.

2.2 Data Acquisition

To perform mapping a 45-watt quartz-halogen tungsten coiled filament calibrated lamp, supplied by Gooch & Housego, was used. The spectral irradiance of the lamp can be seen in figure 2. This calibrated lamp was adapted to a programmable translation system, supplied by Arrick Robotics, which went through a perimeter that covered the entire area of the telescope in adjustable steps by a stepper motor.

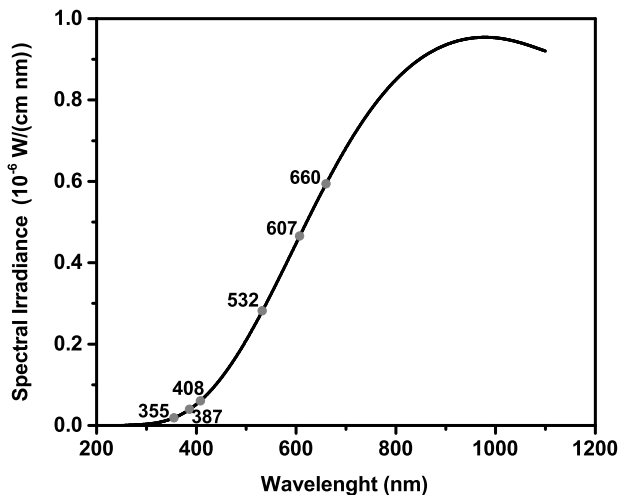


Figure 2. Spectral irradiance of calibrated lamp used for the mapping.

A 12x12 virtual matrix was used to discretize the area of the telescope, shown in figure 1, and using the photon counting (PC) mode of the detected signal it was possible to analyse the spectral response of the optical system. The measurement sequence was designed forming a zig-zag performing 10-second measurements at each matrix cell.



Figure 3. System configuration for different days. On the left, for the day 01/16/2014, it can be seen the the metal structure which caused the stray light. On the right, the same metal structure was covered with a black cloth in order to solve the problem.

To analyze data, it was just added together the absolute values of the PC mode column for each channel, in each cell of the matrix.

3. RESULTS

Figure 4 shows the first results for the day 01/16/2014. During the measurements, we did not take care about the potential sources of stray light as the metal support fixed in the telescope that could be seen in figure 3, on the left. The stray light effect can be seen in five of the six channels, it does not appear only for the 355 channel. This can be explained by the low photon count in this channel.

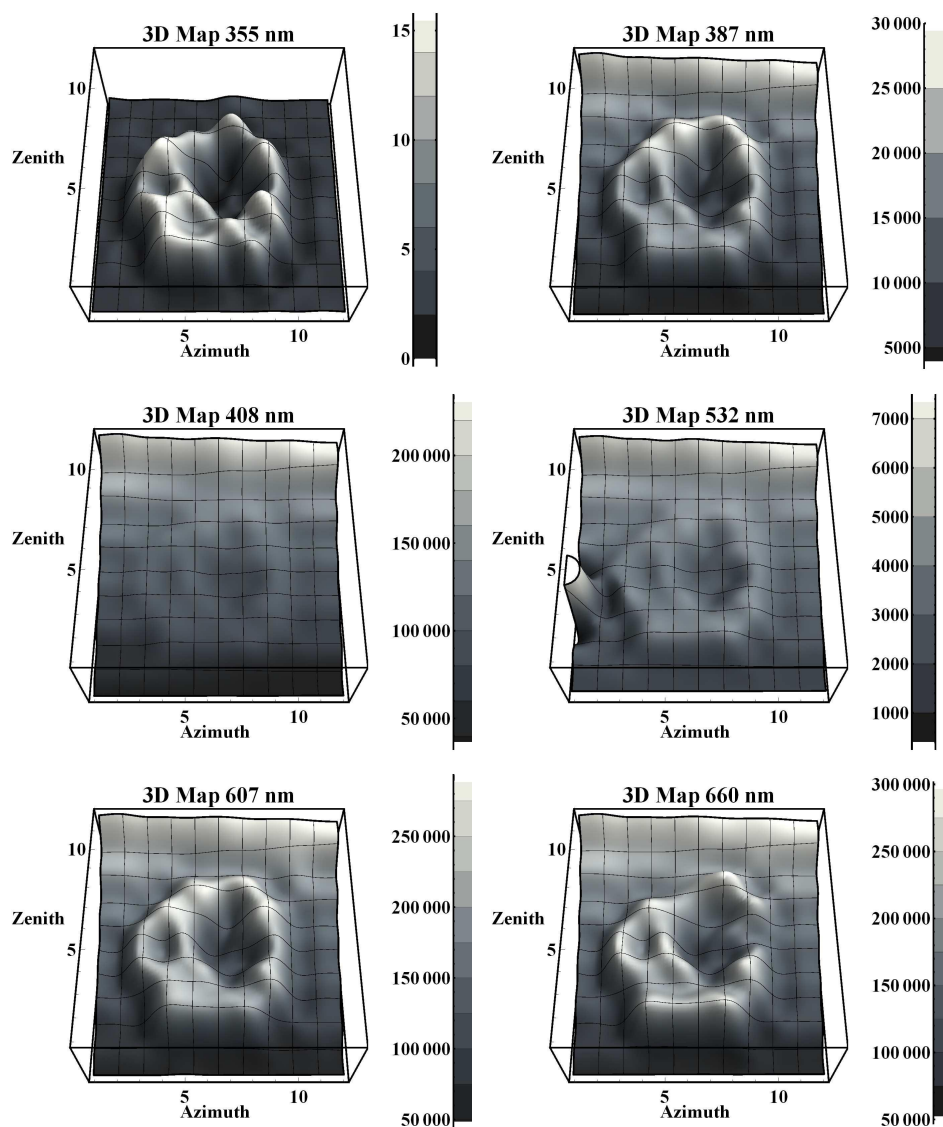


Figure 4. Mapping results for the day 01/16/2014.

In order to solve the problem exposed in figure 4, we just covered the metal support with a black cloth as shown in figure 3, on the right. Figure 5 shows the results for this new mapping carried out in 01/22/2014. Now it is possible to verify a misalignment of the filter on channel 532, since the signal in this channel shows a low count in the upper side at the area of the telescope. Because this effect happens only on channel 532, it was discarded the hypothesis of a misalignment of the telescope mirror, otherwise all the others channels should present such issue.

After these first two mappings, an effort was made to verify the efficiency of transmission of filters by setting up their transmission spectrum and, thus, allowing better optimization of the system. Figure 6 shows the last

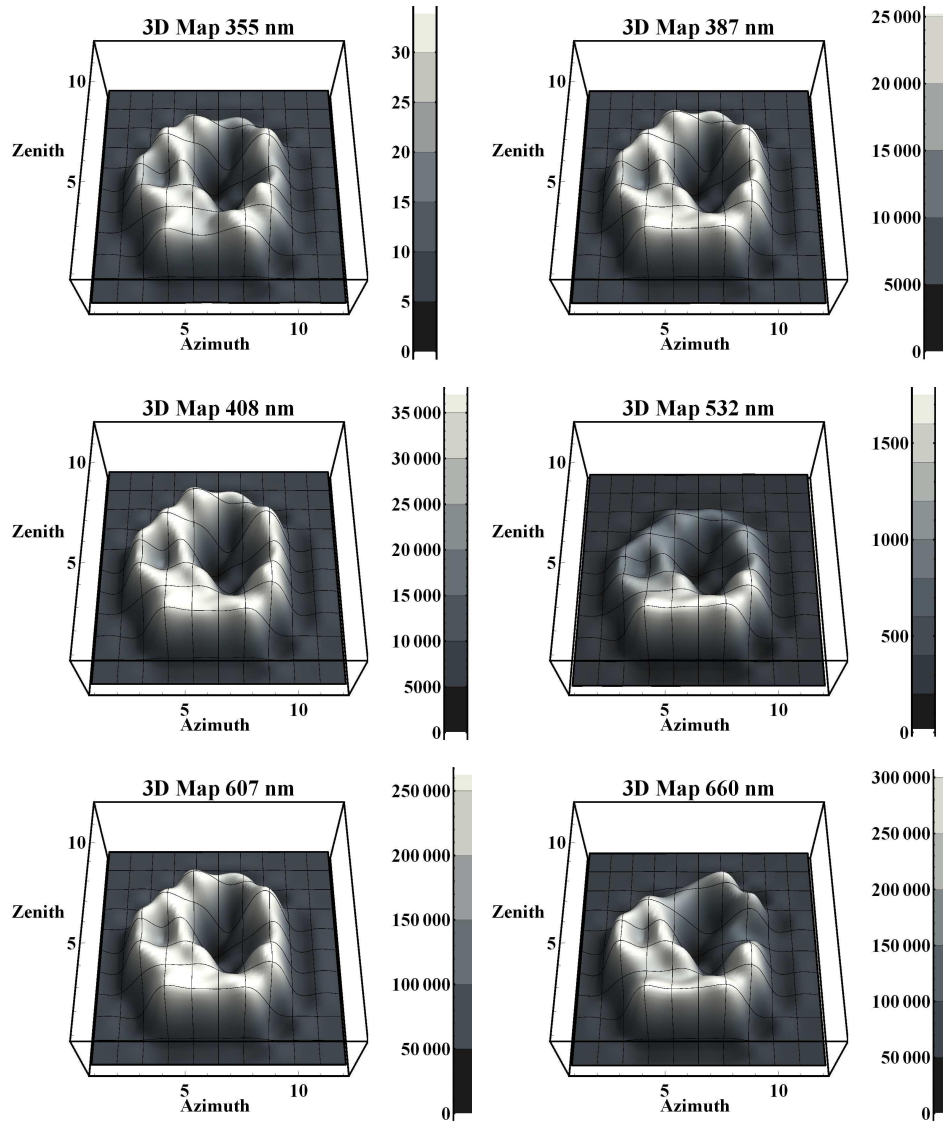


Figure 5. Mapping results for the day 01/22/2014.

results, after all optimization, carried out in 04/09/2014. Here is possible to see an uniformity in the spectral response of the optical system, for most channels. There is only one exception for channel 660, which could represent a failure in the response of PMT.

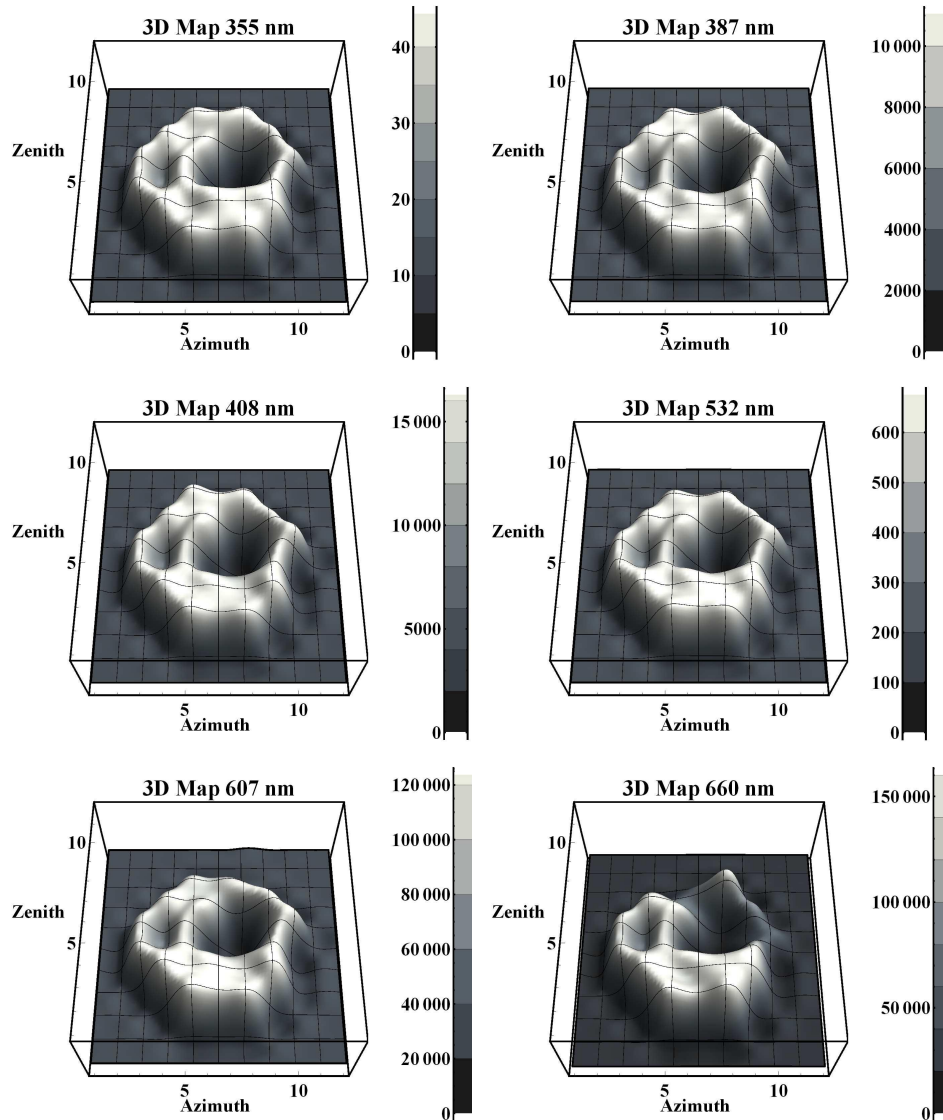


Figure 6. Mapping results for the day 04/09/2014.

4. CONCLUSIONS

This study was performed in a 3-step sequence. First we scanned the area of the telescope without worrying about any kind of issue and using the same setup system had been used to make measurements since then. During this first scanner, it was detected a stray light which came through the metal support of the mirror fixed to the telescope. After correcting this issue, it was made a second scanner which allowed us to identify a misalignment in 532 channel. The third step scanner was performed after optimizing the whole optical system in order to get the best SNR.

The optical characterization of the system, using a reference tungsten lamp, carried out in this study proved an useful tool to identify any possible distortions in the interference filters, telescope mirror and stray light contamination. The results showed the potential that mapping methodology has to help lidars developers to solve issues in the optical system.

ACKNOWLEDGMENTS

The authors would like to thank the supporting agencies Coordenação de Aperfeiçoamento de Pessoal de Nível Superior (CAPES), Conselho Nacional de Desenvolvimento e Pesquisa (CNPq), Fundação de Amparo à Pesquisa do Estado de São Paulo (FAPESP) through the projects 2006/02092-6, 2008/58104-8, 2009/14758-7, 2009/16001-0, 2011/14365-5, 2011/00769-7 and Comissão Nacional de Energia Nuclear (CNEN) for financing the research.

REFERENCES

1. S. H. Melfi, D. N. Whiteman, and R. Ferrare, "Observation of Atmospheric Fronts Using Raman Lidar Moisture Measurements," *Journal of Applied Meteorology* **28**(9), pp. 789–806, 1989.
2. D. N. Whiteman, S. H. Melfi, and R. A. Ferrare, "Raman Lidar System for the Measurement of Water-Vapor and Aerosols in the Earths Atmosphere," *Applied Optics* **31**(16), pp. 3068–3082, 1992.
3. K. D. Evans, S. H. Melfi, R. A. Ferrare, and D. N. Whiteman, "Upper tropospheric temperature measurements with the use of a Raman lidar," *Applied Optics* **36**(12), pp. 2594–2602, 1997.
4. D. Mueller, I. Mattis, A. Ansmann, U. Wandinger, and D. Althausen, "Raman lidar for monitoring of aerosol pollution in the free troposphere," in *Advanced Environmental Monitoring*, Kim, YJ and Platt, U, ed., pp. 155–166, 2008. 6th International Symposium on Advanced Environmental Monitoring, Heidelberg, Germany, Jun 27-30, 2006.
5. A. Ansmann, M. Riebesell, and C. Weitkamp, "Measurement of Atmospheric Aerosol Extinction Profiles With a Raman Lidar," *Optics Letters* **15**(13), pp. 746–748, 1990.
6. G. Vaughan, D. P. Wareing, L. Thomas, and V. Mitev, "Humidity measurements in the free troposphere using raman backscatter," *Quarterly Journal of the Royal Meteorological Society* **114**(484), pp. 1471–1484, 1988.
7. V. Sherlock, A. Hauchecome, and J. Lenoble, "Methodology for the independent calibration of raman backscatter water vapor lidar systems," *Applied Optics* **38**, pp. 5816–5837, 1999.
8. D. N. Whiteman, "Examination of the traditional raman lidar technique. i. evaluating the temperature-dependent lidar equations," *Applied Optics* **42**(15), pp. 2571–2592, 2003.
9. D. D. Venable, D. N. Whiteman, M. N. Calhoun, A. O. Dirisu, R. M. Connell, and E. Landulfo, "Lamp mapping technique for independent determination of the water vapor mixing ratio calibration factor for a raman lidar system," *Applied Optics* **40**, pp. 4622–4632, 2011.
10. E. Landulfo, R. F. Da Costa, A. S. Torres, F. J. S. Lopes, D. N. Whiteman, and D. D. Venable, "Raman water vapor lidar calibration," *Proc. SPIE* **7479**, pp. 74790J–74790J–9, 2009.
11. T. Leblanc and I. S. McDermid, "Accuracy of raman lidar water vapor calibration and its applicability to long-term measurements," *Applied Optics* **47**, pp. 5592–5603, 2008.
12. T. Leblanc and I. S. McDermid, "Reply to "Comments on Accuracy of Raman lidar water vapor calibration and its applicability to long-term measurements" by Whiteman et al.," *Applied Optics* **50**(15), pp. 2177–2178, 2011.
13. D. N. Whiteman, M. Cadirola, D. Venable, M. Calhoun, L. Miloshevich, K. Vermeesch, L. Twigg, A. Dirisu, D. Hurst, E. Hall, A. Jordan, and H. Voemel, "Correction technique for Raman water vapor lidar signal-dependent bias and suitability for water vapor trend monitoring in the upper troposphere," *Atmospheric Measurement Techniques* **5**(11), pp. 2893–2916, 2012.
14. J. A. Cooney, "Measurement of the ratio of the vibrational raman cross section for H_2O vapor to the nitrogen vibrational-rotational raman band," *Spectroscopy Letters* **3**(11&12), pp. 305–309, 1970.
15. C. M. Penney and M. Lapp, "Raman-scattering cross sections for water vapor," *Journal of the Optical Society of America* **66**(5), pp. 422–425, 1976.
16. G. Avila, J. M. Fernandez, B. Mate, G. Tejada, and S. Montero, "Re-vibrational Raman cross sections of water vapor in the OH stretching region," *Journal of Molecular Spectroscopy* **196**(1), pp. 77–92, 1999.
17. M. Adam, "Notes on Rayleigh scattering in lidar signals," *Applied Optics* **51**(12), pp. 2135–2149, 2012.
18. B. Thomas, A. Miffre, G. David, J. P. Cariou, and P. Rairoux, "Remote sensing of trace gases with optical correlation spectroscopy and lidar: theoretical and numerical approach," *Applied Physics B* **108**(3), pp. 689–702, 2012.

19. B. Thomas, G. David, C. Anselmo, J.-P. Cariou, A. Miffre, and P. Rairoux, "Remote sensing of atmospheric gases with optical correlation spectroscopy and lidar: first experimental results on water vapor profile measurements," *Applied Physics B* **113**(2), pp. 265–275, 2013.
20. B. Thomas, G. David, C. Anselmo, E. Coillet, K. Rieth, A. Miffre, J.-P. Cariou, and P. Rairoux, "Remote sensing of methane with broadband laser and optical correlation spectroscopy on the Q-branch of the 2 ν_3 band," *Journal of Molecular Spectroscopy* **291**(SI), pp. 3–8, 2013.
21. E. Landulfo, A. Papayannis, P. Artaxo, A. D. A. Castanho, A. Z. de Freitas, R. F. Souza, N. D. V. Junior, M. Jorge, O. R. Sanchez-Ccoyllo, and D. S. Moreira, "Synergetic measurements of aerosols over são paulo, brazil using lidar, sunphotometer and satelite data during dry season.," *Atmospheric Chemistry and Physics* **3**, pp. 1523–1539, 2003.
22. E. Landulfo, A. Papayannis, P. Artaxo, A. D. A. Castanho, A. Z. de Freitas, R. F. Souza, N. D. V. J. M. Jorge, O. R. Sánchez-Ccoyllo, and D. S. Moreira, "Tropospheric aerosol observations in são paulo, brazil using a compact lidar system," *Int. J. Rem. Sens.* **26**, pp. 2797–2816, 2005.